Supporting Information

Rational Construction of VSe$_2$ Encapsulated in Selenized Polyacrylonitrile toward High-rate Capacity and Wide Temperature Tolerance for Potassium-ion Batteries

*Lihong Xu[a], Jiefeng Ye[c], Wenti Guo[c], Tingjie Chen[a], Xiaochuan Chen[*b], Qingrong Qian[b, e], JianMin Zhang[*c], Mingdeng Wei[d], Xiangfang Peng[*a] and Lingxing Zeng[*b, e]*

a College of Materials Science and Engineering, Key Laboratory of Polymer Materials and Products of Universities in Fujian, Fujian University of Technology, Fuzhou 350002 PR China.
b Engineering Research Center of Polymer Green Recycling of Ministry of Education, College of Environmental and Resources, Fujian Normal University, Fuzhou 350007 PR China.
c Fujian Provincial Key Laboratory of Quantum Manipulation and New Energy Materials College of Physics and Energy, Fujian Normal University, Fuzhou 350117 PR China.
d Fujian Provincial Key Laboratory of Electrochemical Energy Storage Materials, Fuzhou University, 350002 PR China.
e Key Laboratory of Advanced Energy Material s Chemistry (Ministry of Education), College of Chemistry, Nankai University, Tianjin 300071 PR China.

Corresponding Author

*X. Chen. E-mail: chenxiaocuan@fjnu.edu.cn   Tel/Fax: 86 591 83465156.

*J. Zhang. E-mail: jmzhang@fjnu.edu.cn.

*X. Peng. E-mail: pengxf@fjut.edu.cn.

*L. Zeng. E-mail: zenglingxing@fjnu.edu.cn.

1. Experimental Section

1.1 Preparation of VSe₂/SePAN

The preparation of VSe$_2$/SePAN is shown in **Fig. 1**. First, the mass of 0.8 g VO(acac)$_2$ (99%, Aladdin) was completely dispersed in 10 mL solvent of DMF (99.0%, Sinopharm Group Chemical Reagent Co., Ltd.) and mixed with 0.5 g of PAN (M$_W$=150000, Sigma) under magnetic stirring for 24 h at room temperature to obtain homogeneous precursor polymer solution. After that, the above solution was poured into a syringe with volume of 10 mL. A high-voltage power supply was connected to the needle. The electrospinning environment was maintaining at feeding speeds of 0.5 mL h^{-1} and a set voltage of 22 kV. Aluminum foil attached on the disc was employed as fiber collector. And the spinning distance between the needle tip and collector was fixed at 15 cm. Then the obtained precursor VO(acac)$_2$/PAN fiber membrane was dried at 60 °C in a vacuum oven for 12 h, which was cut into a small round shape with a diameter of around 1 cm.

Next, in order to achieved selenized polyacrylonitrile nanofibers incorporating VSe$_2$ (VSe$_2$/SePAN), heat treatment was carried out for fiber membrane. Specifically, the collected VO(acac)$_2$/PAN fiber with selenium powders (w:w=1:2) sealed in a quartz tube was calcined at 350 °C for 5 h with a ramp rate of 2 °C/min under argon flow and then further increased to 500 °C for 2 h with a heating rate of 5 °C/min, which allow the simultaneous selenylation of VO(acac)$_2$ and PAN in the fiber mat.

1.2 Material characterization

The investigation of the crystal structure and morphology of the obtained samples

was carried out by X-ray diffraction (XRD, D8-Advance) and scanning electron microscopy (SEM, Hitachi 8100). The TEM and HRTEM images were recorded using transmission electron microscopy (TEM, FEI). The crystal structure of VSe_2 quantum dots was studied using high-angle annular dark-field scanning transmission electron microscopy (HAADF-STEM, FEI Themis z 200 kV). Raman spectrometer (Raman, DXR2xi) and X-ray photoelectron spectroscopy (XPS, ESCALAB MARK II) were utilized to study the surface chemical species. Thermogravimetric test (TA Q50) was conducted in airflow from 30 to 700 °C with 10 °C min^{-1} of temperature ramp. Solid-phase nuclear magnetic resonance spectra (13C NMR, Bruker Avance III 400 WB) were performed equipped with a CP/MAS probe.

1.3 Electrochemical measurements

The electrochemical measurement of all electrodes were tested using CR2025-type coin cells in a high-purity Ar atmosphere glove box (H_2O, O_2, <0.1 ppm). The preparation of electrode slurry was carried out by uniformly combining the VSe_2/SePAN composite active material, super-P conducting agent, and the carboxymethyl cellulose (CMC) binder in deionized water (mass ratio 80:10:10). After being casted onto Cu foil, the slurry was vacuum dried at 80 °C for 10 h. There was ca. 0.8~1.0 mg cm^{-2} of average mass loading on each Cu foil. The glass fiber and potassium metal served as separators and counter electrodes, respectively. Meanwhile, a 3 M potassium bis(fluoroslufonyl)imide (KFSI) solution in dimethyl ether (DME) was employed as an electrolyte. The potassium-ion hybrid capacitors (PIHC, VSe_2/SePAN//AC) were constructed by using VSe_2/SePAN anode and active carbon

(AC) cathode with a weight ratio of 1:3. Thereinto, cathode AC electrodes were made by combining NMP with 80 wt% AC, 10 wt% of both conductive carbon and PVDF binder followed by even coating of the resulting mixture onto aluminum foils, which was then subsequently dried overnight in a vacuum oven at 80 °C. In half-batteries, the PIHC pre-assembly anodes were cycled five times and discharged to 0.01 V at 0.1 A g^{-1}. The Ivium electrochemical workstation was used to conduct cyclic voltammetry (CV, 0.01-3.0 V) and impedance spectroscopy (EIS, 100 kHz to 10 mHz). Experiments utilizing the galvanostatic intermittent titration technique (GITT) were conducted in either a 15 min of charged or discharged state at 50 mA g^{-1} pulse current, followed by a 180 min of pulse relaxation interval. The mass of the active substance was used in all calculations of reversible specific capacities.

1.4 Density Functional Theory Calculation

The theoretical computations in this work were performed using the Vienna ab initio simulation software (VASP),[S1,2] which is based on density functional theory (DFT). The projector augmented wave (PAW) pseudopotential was employed.[S3] Within the framework of the generalized gradient approximation (GGA), the Perdew-Burke-Ernzerhof (PBE) functional was used for the electron exchange-correlation interactions.[S4] The graphene with a space group of P6/mmm (No. 191) with a = b = 2.47 Å lattice constants were used. A monolayer graphene primitive cell 4×4 was constructed to create a stable monolayer doping substrate. The space group of VSe_2 and K_2Se were P m1 (No.164) and Fm m (No.225), respectively. Maximum residual forces acting on individual atoms must be less than 0.01 eV/Å, and the overall energy

must converge to 105 eV, to complete the geometric optimization. The cutoff energy for the plane-wave basis was determined to be 520 eV. A gamma-centered 4×4×1 k-mesh was used to sample the Brillouin zone for the graphene adsorption system. A 20 Å vacuum layer was applied in the z-direction. Using the optB88-vdW method, the van der Waals forces between graphene and adsorbed atoms were corrected.[S5]

2. Supplementary Figures and Tables

Table S1 Comparison of potassium storage properties of various vanadium selenides anode materials

Anode Materials	Reversible capacity (mAh g^{-1})	Cycling stability (n)	Rate capability (mAh g^{-1})	Ref.
VSe$_2$ ultrathin nanosheets	335 (0.1 A g^{-1})	200	172 (2 A g^{-1})	[S6]
	169 (2 A g^{-1})	500		
VSe$_2$@PPy	203 (0.5 A g^{-1})	80	148.6 (5 A g^{-1})	[S7]
VSe$_2$/MXene	302.4 (0.2 A g^{-1})	200	106.9 (2 A g^{-1})	[S8]
	138.7 (1 A g^{-1})	500		
VSe$_2$@CQDs	362 (0.1 A g^{-1})	200	255 (2 A g^{-1})	[S9]
VSe$_2$@CNB	227.4 (0.1 A g^{-1})	100	134 (1 A g^{-1})	[S10]
	125 (0.5 A g^{-1})	1000		
NP-V$_3$Se$_4$/CNFs	311 (0.1 A g^{-1})	50	231 (2 A g^{-1})	[S11]
	207 (2 A g^{-1})	800		
VSe$_{1.5}$/CNFs	313 (0.1 A g^{-1})	40	141 (2 A g^{-1})	[S12]
	177 (1 A g^{-1})	100		
VSe$_2$/SePAN	**481 (0.1 A g^{-1})**	**50**	**255 (2 A g^{-1})**	**This work**
	206 (2 A g^{-1})	**300**	**188 (5 A g^{-1})**	

Ref.

[S1] G. Kresse and J. Hafner, Ab initio molecular dynamics for open-shell transition metals, *Phys. Rev. B,* 1993, **48**, 13115-8.

[S2] G. Kresse and J. Furthmuller, Efficient iterative schemes for ab initio total-energy calculations using a plane-wave basis set, *Phys. Rev. B,* 1996, **54**, 11169-86.

[S3] PE Blöch, Projector augmented-wave method, *Phys Rev B,* 1994, **50**, 17953.

[S4] J. P. Perdew, K. Burke and M. Ernzerhof, Generalized gradient approximation made simple, *Phys. Rev. Lett.,* 1996, **77**, 3865.

[S5] J. Klimeš, D. R. Bowler and A. Michaelides, Chemical accuracy for the van der Waals density functional, *J. Phys-Condens. Mat.,* 2009, **22**, 022201.

[S6] C. Yang, J. Feng, F. Lv, J. Zhou, C. Lin, K. Wang, Y. Zhang, Y. Yang, W. Wang, J. Li and S. Guo, Metallic graphene-like VSe_2 ultrathin nanosheets: superior potassium-ion storage and their working mechanism, *Adv. Mater.,* 2018, **30**, 1800036.

[S7] Y. Yi, X. Du, Z. Zhao, Y. Liu, H. Guan, X. Liu, X. Pei, S Zhang and D. Li, Coupling of metallic VSe_2 and conductive polypyrrole for boosted sodium-ion storage by reinforced conductivity within and outside, *ACS Nano,* 2022, **16**, 7772-7782.

[S8] H. Zhang, D. Xiong, C. Xu, Y. Xie, L. Zeng, Z. Feng, M. He and Q. Liu, VSe_2/MXene composite with hierarchical three-dimensional structure encapsulated in dopamine as an anode for potassium-ion batteries, *Electrochim. Acta,* 2022, **421**, 140487.

[S9] Y. Feng, C. Xu, K. Wu, Y. Guo, S. Wu, Z. Guo, M. He and M. Xue, Carbon quantum dot-coated VSe_2 nanosheets as anodes for high-performance potassium-ion batteries, *ACS Appl. Nano Mater.,* 2022, **5**, 13136-13148.

[S10] Y. Feng, K. Wu, C. Xu, S. Wu, Z. Guo, M. He, X. Xu and M. Xue, Cellulose/lignin-based carbon nanobelt aerogels coating on VSe_2 nanosheets as anode for high performance potassium-ion batteries, *J. Power Sources,* 2022, **548**, 232033.

[S11] L. Xu, W. Guo, L. Zeng, X. Xia, Y. Wang, P. Xiong, Q. Chen, J. Zhang, M. Wei and Q. Qian, V_3Se_4 embedded within N/P co-doped carbon fibers for sodium/potassium ion batteries, *Chem. Eng. J.,* 2021, **419**, 129607.

[S12] L. Xu, P. Xiong, L. Zeng, Y. Fang, R. Liu, J. Liu, F. Luo, Q. Chen, M. Wei and Q. Qian, Electrospun $VSe_{1.5}$/CNF composite with excellent performance for alkali metal ion batteries, *Nanoscale,* 2019, **11**, 16308-16.
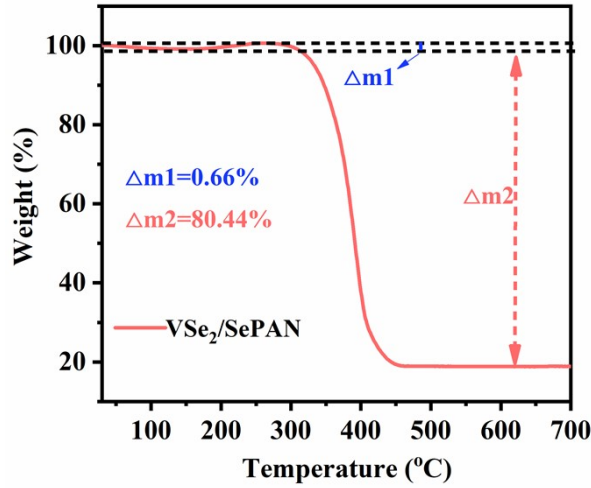
Fig. S1 TG curve of VSe$_2$/SePAN composite in air.

TG experiment is conducted in the range of 30 ~ 700 °C under air atmosphere, as exhibited by the results in **Fig. S1**. The primary weight loss below 180 °C can be attributed to the evaporation of evaporation of absorbed water. After that, there is a slight curve rise in sample at 180-300 °C, which is contributed to the oxidation of VSe$_2$ into V$_2$O$_5$ and SeO$_2$. Subsequently, the distinct weight loss can be observed between 300-460 °C, corresponding to the sublimation of SeO$_2$ and the combustion oxidation of carbon. Therefore, the content of VSe$_2$ in VSe$_2$/SePAN composite was determined to be ≈43.7%.

$$2VSe_2 + 13/2O_2 \rightarrow V_2O_5 + 4SeO_2$$
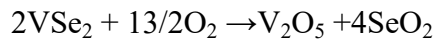
For VSe$_2$/SePAN, the VSe$_2$ content (wt%) can be calculated as

$$VSe_2(\%)=100\% \times 2 \times (M_{VSe2}/M_{V2O5}) \times (W_{remain} V_2O_5/W_{100}°) = 100\% \times 2 \times (208.86/181.88)$$
$$\times (18.9)/99.34\% \approx 43.7\%$$
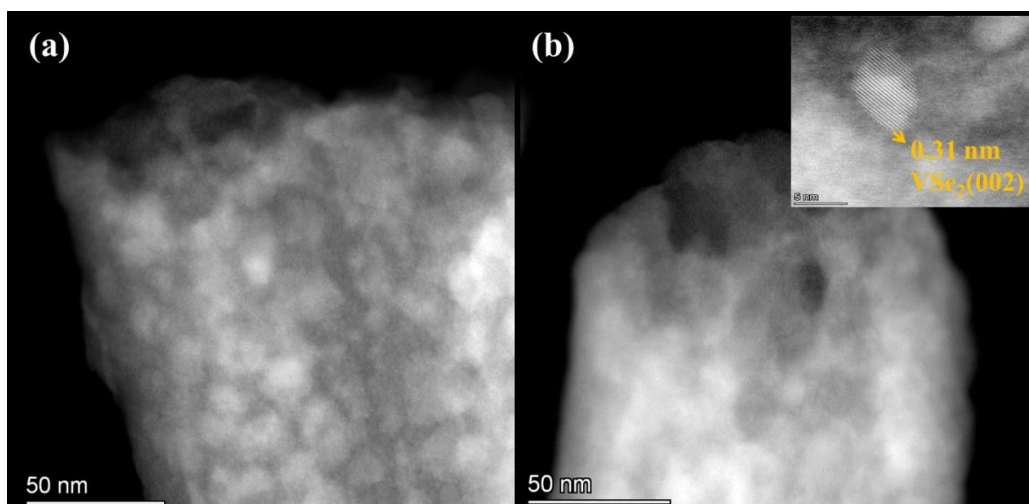
Fig. S2 HAADF-STEM images of VSe$_2$/SePAN composite.
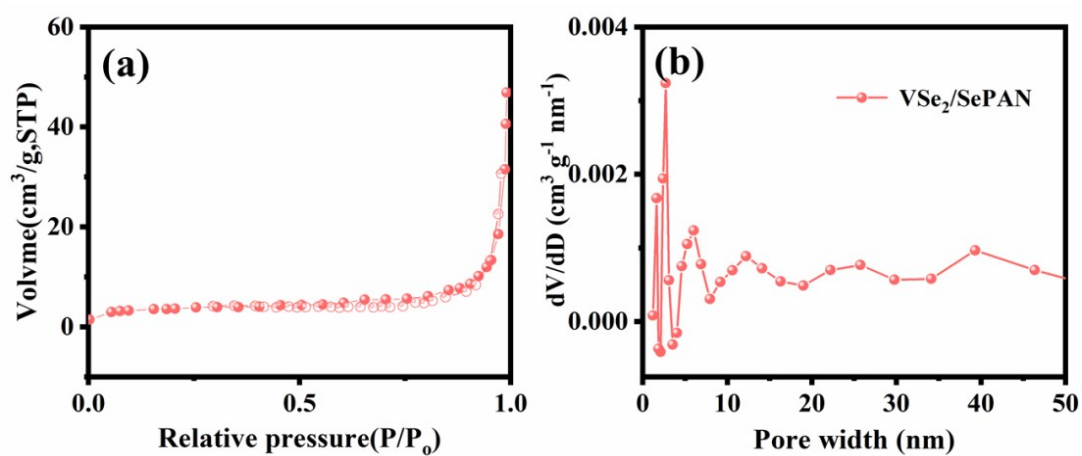

Fig. S3 (a) Nitrogen adsorption-desorption isotherms of VSe$_2$/SePAN composite. (b)
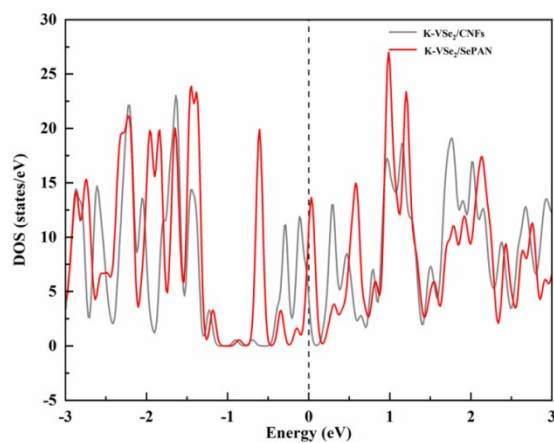
Pore size distribution.

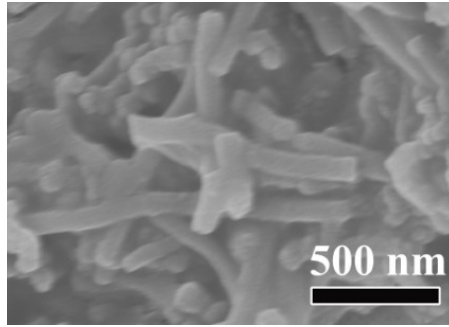**Fig. S4** The corresponding total DOS of K-VSe$_2$/SePAN and K-VSe$_2$/CNFs.

Fig. S5 SEM image of VSe$_2$/SePAN electrode after 100 cycles at 2 A g^{-1} for PIBs.
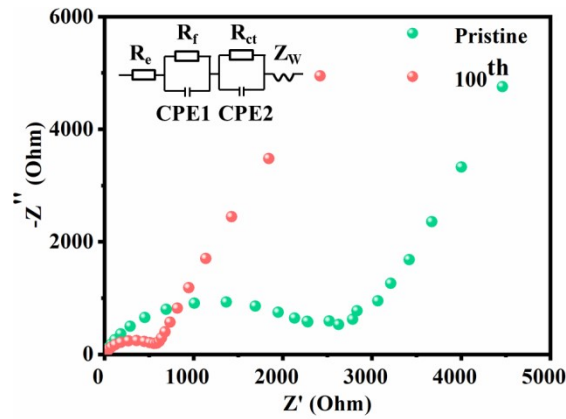

Fig. S6 Nyquist plots of the VSe$_2$/SePAN electrode; inset is the corresponding equivalent circuit according to fit the results. Re reflects the resistance of electrolyte. The semicircle at the medium/high frequency region is the impedance of the SEI film (R$_f$) and the charge-transfer impedance (R$_{ct}$). CPE is a constant-phase element of the electrolyte and electrode interface. The inclined line in low frequency region is Warburg impedance (Zw).

The diffusion coefficients of K ions (D$_{K+}$) are calculated with the help of the following equation:

$$\mathbf{D}_{K+} = \frac{4}{\pi\,\tau}\left(\frac{m_B V_M}{M_b S}\right)^2\left(\frac{\Delta E_s}{\Delta E\tau}\right)^2$$

τ: Constant current pulse time.

m_B: mass of the active material.

V_M: molar volume of active electrode materials.

M_B：molar mass of carbon.

S: The area of the electrode materials.

ΔE_s: The potential change of steady state caused by current pulse.

ΔE_t: The potential change during the constant current pulse after eliminating the iR drop.
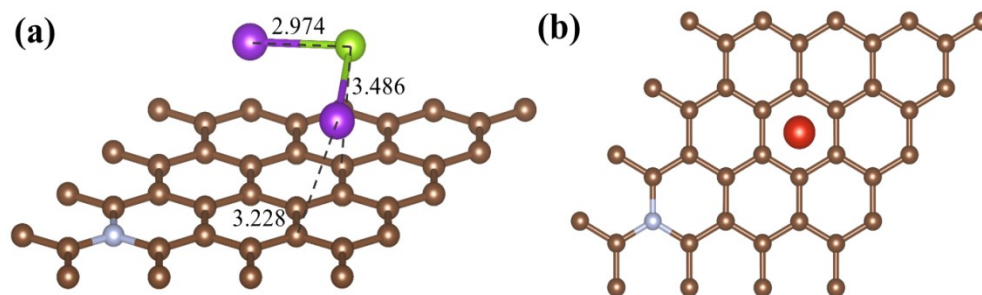

Fig. S7 (a) K_2Se and (b) V atom adsorbed on pristine graphene, respectively, after geometry optimization.